Mineralogical Magazine (2019), **83**, 821–827
doi:10.1180/mgm.2019.59

CAMBRIDGE UNIVERSITY PRESS

Article

Bavsiite, $Ba_2V_2O_2[Si_4O_{12}]$, mineral data and crystal structure

Hans-Peter Bojar[1]*, Franz Walter[1] and Judith Baumgartner[2]

[1]Universalmuseum Joanneum, Centre of Natural History, Weinzöttlstraße 16, A-8045 Graz, Austria; and [2]Institute of Inorganic Chemistry, Technical University of Graz, Stremayrgasse 16/IV, A–8010 Graz, Austria

Abstract

Bavsiite from the type locality Gun Claim, Yukon Territory, Canada, occurs as millimetre-sized sky-blue platy crystals in a barium-rich low-temperature skarn related to a porphyritic quartz monzonite stock. Associated minerals are alstonite, baryte, celsian, diopside, fresnoite, mica, suzukiite, walstromite, witherite and minerals of the cerchiaraite group. Bavsiite is optical uniaxial (+), with $\omega = 1.725(3)$ and $\epsilon = 1.750(3)$ (589 nm) and pleochroic. Electron microprobe analyses yielded the empirical formula $Na_{0.02}Ba_{1.98}Ti_{0.16}Fe^{2+}_{0.03}V^{4+}_{1.80}Al_{0.05}Si_{4.00}O_{14}$ based on 14 oxygen atoms, the simplified chemical formula is $Ba_2V_2Si_4O_{14}$. Bavsiite is tetragonal, space group $I4/m$, $a = 7.043(1)$, $c = 11.444(2)$ Å and $Z = 2$ obtained from single crystal data at 100 K, which are in good agreement with cell parameters from powder diffraction data at 293 K: $a = 7.051(1)$ Å and $c = 11.470(1)$ Å. The eight strongest lines of the powder X-ray diffraction pattern are [*d*, Å (*I*,%)(*hkl*)]: 3.76(30)(112), 3.36(44)(013), 3.004(100)(022), 2.493(43)(220), 2.486(67)(114), 2.286(24)(222), 1.785(39)(116) and 1.763(25)(040). The crystal structure was refined to $R = 0.0159$ based upon 312 unique reflections with $I > 2\sigma(I)$. The crystal structure of bavsiite comprises unbranched single $[Si_4O_{12}]^{8-}$ rings connected by $[VO_5]^{6-}$ square pyramids and BaO_{12} polyhedra. It can also be considered as cage–like $[Si_4V_2O_{18}]^{12-}$ clusters built by four SiO_4 tetrahedra and two VO_5 square pyramids. These clusters are cross–linked to form a pseudo-two-dimensional network (2D) parallel to (001) containing empty channels along the *a* axis and the 2D networks held together by Ba^{2+} ions located in channels parallel to the *c* axis. The structural formula is $Ba_2V_2O_2[Si_4O_{12}]$. Bavsiite is polymorphic to suzukiite, $BaVSi_2O_7$, which is orthorhombic.

Keywords: bavsiite, new mineral, mineral data, crystal structure, Gun Claim, Yukon Territory, Canada

(Received 27 June 2019; accepted 4 September 2019; Accepted Manuscript published online: 12 September 2019; Associate Editor: Ian T. Graham)

Introduction

The Gun Claim (sometimes also written Gunn Claim), Yukon Territory (130°0′51”W, 62°50′50”N), Canada is located ~4 km southeast of Wilson lake and 16 km southeast of Itsy Peak. It is the type locality for itsiite (Kampf *et al.*, 2014), meierite (Peterson *et al.*, 2016), pellyite (Montgomery *et al.*, 1972) and the co-type locality of titantaramellite (Alfors and Pabst, 1984). The mineralisation is a barium-rich low-temperature skarn related to a porphyritic quartz monzonite stock. Skarn bodies have developed in limestone adjacent to the igneous contact. The major mineral assemblage includes andradite, baryte, cerchiaraite, gillespite, pellyite, quartz, sanbornite, taramellite and witherite (Montgomery *et al.*, 1972; MacNeil *et al.*, 2013; Kampf *et al.*, 2014).

Occurrence and physical properties

Bavsiite has been approved by the Commission on New Minerals, Nomenclature and Classification of the International Mineralogical Association (IMA2014-019, Bojar and Walter, 2014) and the type specimen is hosted in the mineralogical collection of the Universalmuseum Joanneum Graz, Austria (catalogue number 85.282). Bavsiite and suzukiite, which have nearly the same chemical composition, were found in a white, marble-like skarn-type rock. Bavsiite (Fig. 1) occurs as sky-blue, platy crystals up to 0.3 mm across with a thickness of a few hundredth of a millimetre and flattened on {001}. Bavsiite is transparent with a vitreous lustre and is non-fluorescent. The streak is white, the Mohs hardness is ~4 and cleavage parallel to (001) is good. Density was not measured directly due to frequent inclusions in bavsiite. Directly associated minerals are alstonite, baryte, celsian, diopside, fresnoite, mica, suzukiite, walstromite, witherite and minerals of the cerchiaraite group.

The Fourier-transform infrared spectrum was recorded using a Perkin Elmer Spectrum 100 spectrophotometer (ATR diamond cell, resolution 4 cm^{-1}, 20 scans). The infrared spectra for bavsiite and suzukiite are overlaid for comparison and given in Fig. 2. The following bands for bavsiite were observed (in cm^{-1}; s: strong, m: medium, w: weak, sh: shoulder): 1223w, 1068s, 993sh, 916s, 743w, 659s, 584m, 537w, 478s and 427m. The bands in the region from 1200 to 900 cm^{-1} are related to the stretching of Si–O in the SiO_4 tetrahedron and V–O of the VO_5 pyramid. The region of 740 to 400 cm^{-1} is related to the bending modes of the SiO_4 and VO_5 structural elements.

Bavsiite is optical uniaxial (+); its optical constants measured with 589 nm on a spindle stage are $\omega = 1.725(3)$ and $\epsilon = 1.750(3)$, the dispersion is weak with $r > v$. Pleochriosm for ω is medium blue and for ε, pale yellow.

*Author for correspondence: Hans-Peter Bojar, Email: hans-peter.bojar@museum-joanneum.at

Cite this article: Bojar H.-P., Walter F. and Baumgartner J. (2019) Bavsiite, $Ba_2V_2O_2[Si_4O_{12}]$, mineral data and crystal structure. *Mineralogical Magazine* **83**, 821–827. https://doi.org/10.1180/mgm.2019.59

© Mineralogical Society of Great Britain and Ireland 2019

https://doi.org/10.1180/mgm.2019.59 Published online by Cambridge University Press

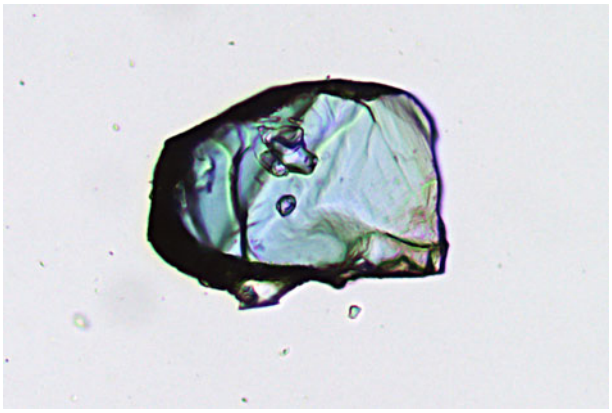


Fig. 1. Transmission-light microscopy image of a single crystal of bavsiite (cat. nr. 85.282). Field of view is 0.2 mm. Photograph: F. Walter.

Table 1. Representative compositions from electron microprobe wavelength dispersive analyses of bavsiite. Average of 10 spot analyses from five crystal fragments.

Constituent	Wt.%	Range	S.D.	Standard
SiO_2	33.40	32.67–34.40	0.47	almandine
TiO_2	1.75	1.07–2.30	0.06	rutile
Al_2O_3	0.33	0.25–0.49	0.02	almandine
FeO	0.30	0.16–0.45	0.02	almandine
VO_2	20.69	20.16–21.39	0.35	V metal
Na_2O	0.08	b.d.l.–0.15	0.02	albite
BaO	42.28	41.52–43.87	0.67	benitoite
Total	98.83			

S.D. – standard deviation; b.d.l. – below detection limit.

Composition

Electron microbeam wavelength dispersive analyses were performed on a Jeol 6610 LV electron microscope equipped with an OXFORD 50 mm^2 energy dispersive and an OXFORD INCA WAVE spectrometer operated at an accelerating voltage of 20 kV and a beam current of 10 nA. Data reduction was done with the *PAP* routine (Pouchou and Pichoir, 1991) implemented in the INCA software of Oxford Instruments. Results of the analyses of bavsiite and minerals of its paragenesis are given in Tables 1 and 2. The empirical formula of bavsiite on the basis of 14 oxygen atoms is: $Na_{0.02}Ba_{1.98}Ti_{0.16}Fe^{2+}_{0.03}V^{4+}_{1.80}Al_{0.05}Si_{4.00}O_{14}$. The simplified chemical formula is $Ba_2V_2Si_4O_{14}$ which requires BaO 43.02, VO_2 23.27 and SiO_2 33.72 wt.%. The elements Ca, Mg, Mn and Sr were also measured, but found to be below the detection limits. The chemical composition of suzukiite and its empirical formula is very close to that of bavsiite: $Na_{0.02}Ba_{1.94}Ti_{0.12}Fe^{2+}_{0.03}V^{4+}_{1.85}Al_{0.04}Si_{4.01}O_{14}$.

Associated feldspars are very low in Ca and high in Ba with higher Ba content in their cores. Fresnoite analyses ($Na_{0.02}Ca_{0.02}Ba_{0.96}Fe^{2+}_{0.01}V^{4+}_{0.22}Ti_{0.79}Al_{0.01}Si_{1.98}O_8$) yielded considerable V^{4+} (tetravalence from stoichiometric considerations) values.

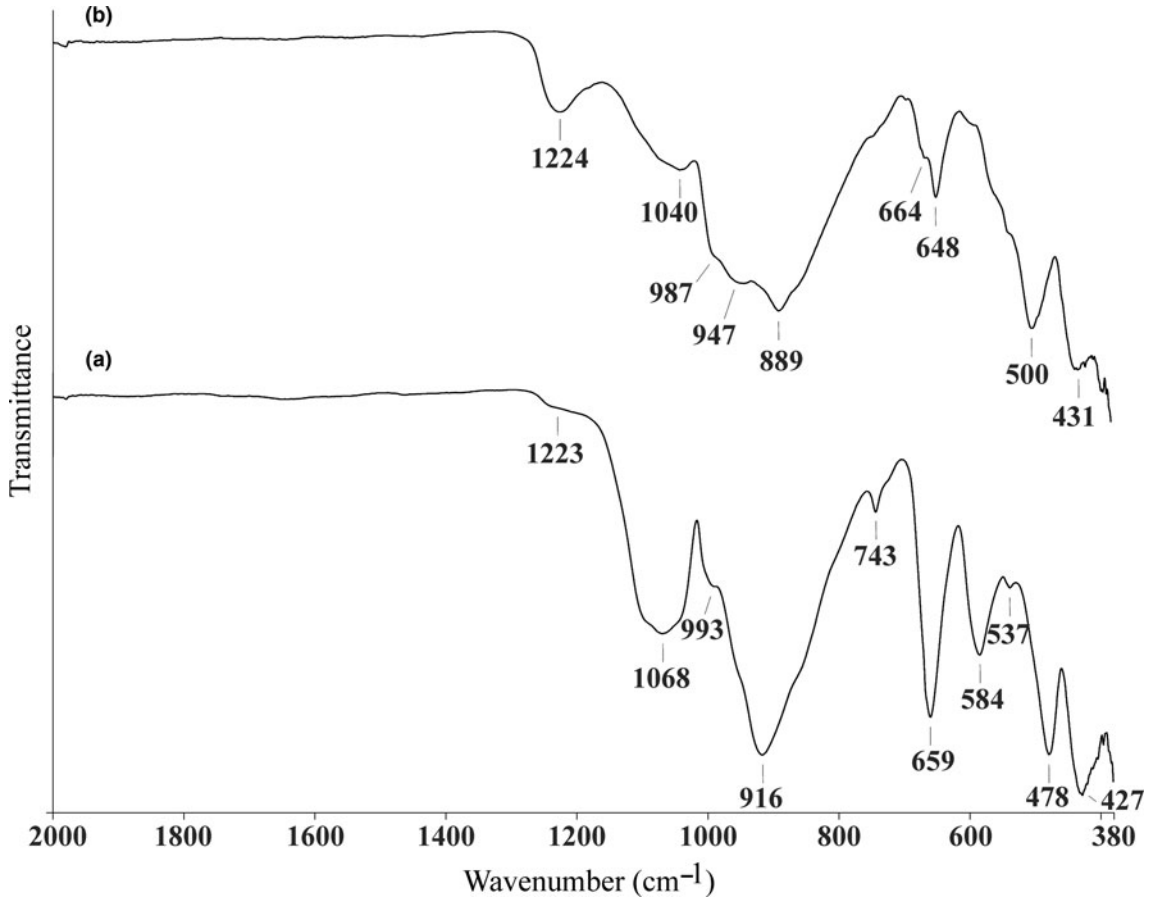


Fig. 2. The Fourier-transform infrared ATR spectra of bavsiite (*a*) and of suzukiite (*b*).

https://doi.org/10.1180/mgm.2019.59 Published online by Cambridge University Press

Table 2. Representative electron microprobe results from wavelength-dispersive spectroscopy analyses and formula units for bavsiite and minerals of its paragenesis*.

	Celsian [1]	Walstromite [2]	Fresnoite [3]	Diopside [4]	Bavsiite [5]	Suzukiite [6]
Wt.%						
SiO_2	35.53	40.76	23.99	52.76	33.40	34.14
TiO_2	b.d.l.	0.16	12.77	b.d.l.	1.75	1.35
Al_2O_3	24.29	b.d.l.	0.09	0.05	0.33	0.25
FeO	0.29	b.d.l.	0.13	4.14	0.30	0.29
VO_2	b.d.l.	b.d.l.	3.71	0.45	20.69	21.81
MgO	b.d.l.	b.d.l.	b.d.l.	15.32	b.d.l.	0.02
CaO	0.17	24.40	0.27	24.38	b.d.l.	0.04
SrO	b.d.l.	0.22	0.09	b.d.l.	b.d.l.	b.d.l.
Na_2O	0.10	0.03	0.10	0.13	0.08	0.09
K_2O	2.63	b.d.l.	b.d.l.	b.d.l.	b.d.l.	b.d.l.
BaO	35.88	35.10	60.85	b.d.l.	42.28	42.25
Sum	98.89	100.67	102.00	97.23	98.83	100.24
Atoms per formula unit						
Si	2.18	3.01	1.98	1.99	4.00	4.01
Ti		0.01	0.79		0.16	0.12
Al	1.76		0.01		0.05	0.04
Fe^{2+}	0.02		0.01	0.13	0.03	0.03
V^{4+}			0.22	0.01	1.80	1.85
Mg				0.86		
Ca	0.01	1.93	0.02	0.99		
Sr		0.01				
Na	0.01		0.02	0.01	0.02	0.02
K	0.21					
Ba	0.86	1.02	1.96		1.98	1.94
Sum	5.05	5.98	5.01	3.99	8.04	8.01

*[1] celsian (on the basis of 8 oxygen atoms); [2] walstromite (9 oxygens); [3] fresnoite (8 oxygens); [4] diopside (6 oxygens); [5] bavsiite (14 oxygens, mean value of 10 analyses of 5 crystal fragments); and [6] suzukiite (14 oxygens, mean value of 5 analyses of one crystal fragment),
b.d.l. – below detection limit.

Slightly low analytical sums are caused most probably by a varying probe current.

Powder X-ray diffraction

The powder X-ray diffraction data (Table 3) for bavsiite were obtained at 293 K using a Bruker-AXS D8 diffractometer with Cu*K*α radiation. To minimise the background, the sample was placed on a low-background silicon wafer; an internal standard was not used. Unit-cell parameters, derived from whole pattern fitting (Pawley method) with fundamental parameters using *TOPAS 4.2* software (Bruker-AXS, 2009) are: $a = 7.051(1)$ Å, $c = 11.470(1)$ Å and $V = 570.2(1)$ Å^3, which are in agreement with those obtained from the single-crystal study (see below). Due to the cleavage of bavsiite parallel to (001) and due to the sample preparation, the intensities for (002), (004), (006) and (008) of the observed pattern are too high in comparison to the (00*l*) intensities of the simulated powder pattern, calculated with data from the single-crystal structure refinement (Table 3). In the powder pattern of bavsiite impurities of feldspar, suzukiite and mica are visible (Fig. 3*a*). For comparison, the simulated powder patterns of bavsiite calculated with parameters of the single-crystal structure refinement at 100 K (Fig. 3*b*) and of β-$BaVSi_2O_7$ (Fig. 3*c*) calculated with parameters of the structure refinement from Liu and Greedan (1994) are overlaid. The powder patterns confirm that bavsiite and β-$BaVSi_2O_7$ have the same crystal structure but are polymorphic to suzukiite ($BaVSi_2O_7$, orthorhombic) shown by overlaying the experimental powder pattern of suzukiite crystals from the type locality of bavsiite (Fig. 3*d*).

Table 3. Powder X-ray diffraction data (*d* in Å) for bavsiite.

I_{obs}	I_{calc}	d_{obs}	d_{calc}	*h k l*
2	3	6.009	6.007	0 1 1
107*	9	5.735	5.735	0 0 2
10	10	4.986	4.986	1 1 0
30	**31**	**3.7630**	**3.7627**	**1 1 2**
17	14	3.5258	3.5257	0 2 0
44	**16**	**3.3609**	**3.3610**	**0 1 3**
7	2	3.0398	3.0406	1 2 1
	4		3.0406	2 1 1
100	**100**	**3.0037**	**3.0035**	**0 2 2**
149*	7	2.8670	2.8674	0 0 4
43	**35**	**2.4933**	**2.4930**	**2 2 0**
67	**33**	**2.4860**	**2.4857**	**1 1 4**
24	**17**	**2.2861**	**2.2863**	**2 2 2**
7	3	2.2294	2.2298	1 3 0
	2		2.2298	3 1 0
11	7	2.2245	2.2246	0 2 4
6	2	2.1817	2.1814	0 1 5
11	6	2.0783	2.0782	1 3 2
	6		2.0782	3 1 2
2	<1	1.9278	1.9279	2 3 1
	1	1.9278	1.9279	3 2 1
3*	<1	1.9118	1.9116	0 0 6
6	5	1.8815	1.8814	2 2 4
39	**13**	**1.7852**	**1.7849**	**1 1 6**
25	**14**	**1.7627**	**1.7628**	**0 4 0**
	7		1.7602	1 3 4
	9		1.7602	3 1 4
4	2	1.7412	1.7411	2 3 3
	2		1.7411	3 2 3
3	3	1.6847	1.6850	0 4 2
17	5	1.6807	1.6805	0 2 6
5	4	1.5964	1.5963	3 3 2
6	3	1.5767	1.5767	2 4 0
	3		1.5767	4 2 0
2	<1	1.5610	1.5611	1 4 3
	1	1.5610	1.5611	4 1 3
16	9	1.5203	1.5203	2 4 2
	9		1.5203	4 2 2
7	6	1.5018	1.5017	0 4 4
5	1	1.4540	1.4540	1 2 7
	1		1.4540	2 1 7
21	7	1.4514	1.4513	1 3 6
	6		1.4513	3 1 6
8	5	1.4381	1.4379	3 3 4
106*	3	1.4338	1.4337	0 0 8
2	1	1.3817	1.3816	2 4 4
	<1		1.3816	4 2 4
8	3	1.3783	1.3779	1 1 8
3	1	1.3443	1.3442	1 5 2
	2		1.3442	5 1 2

I_{obs} and d_{obs} from measurement at 293 K (Bruker D8 diffractometer, Cu*K*α radiation); d_{calc} calculated with profile fitting using *TOPAS* 4.2 and $a = 7.051(1)$ Å, $c = 11.470(1)$ Å; I_{calc} calculated with atomic parameters from single-crystal structure refinement of bavsiite.
*I_{obs} due to preferred orientation of the cleavage plane (001). Scaling is based on I_{obs} (022) = 100.
The strongest lines are indicated in bold.

Single-crystal X-ray structure refinement

A pale blue platy crystal of bavsiite (Fig. 1) was used for X-ray single-crystal data collection on a Bruker AXS Smart Apex CCD diffractometer equipped with graphite-monochromatised Mo*K*a radiation (0.71073 Å). The data were recorded with the program *SMART*, integrated with the program *SAINT* up to $\theta_{max} = 26.3°$,

https://doi.org/10.1180/mgm.2019.59 Published online by Cambridge University Press

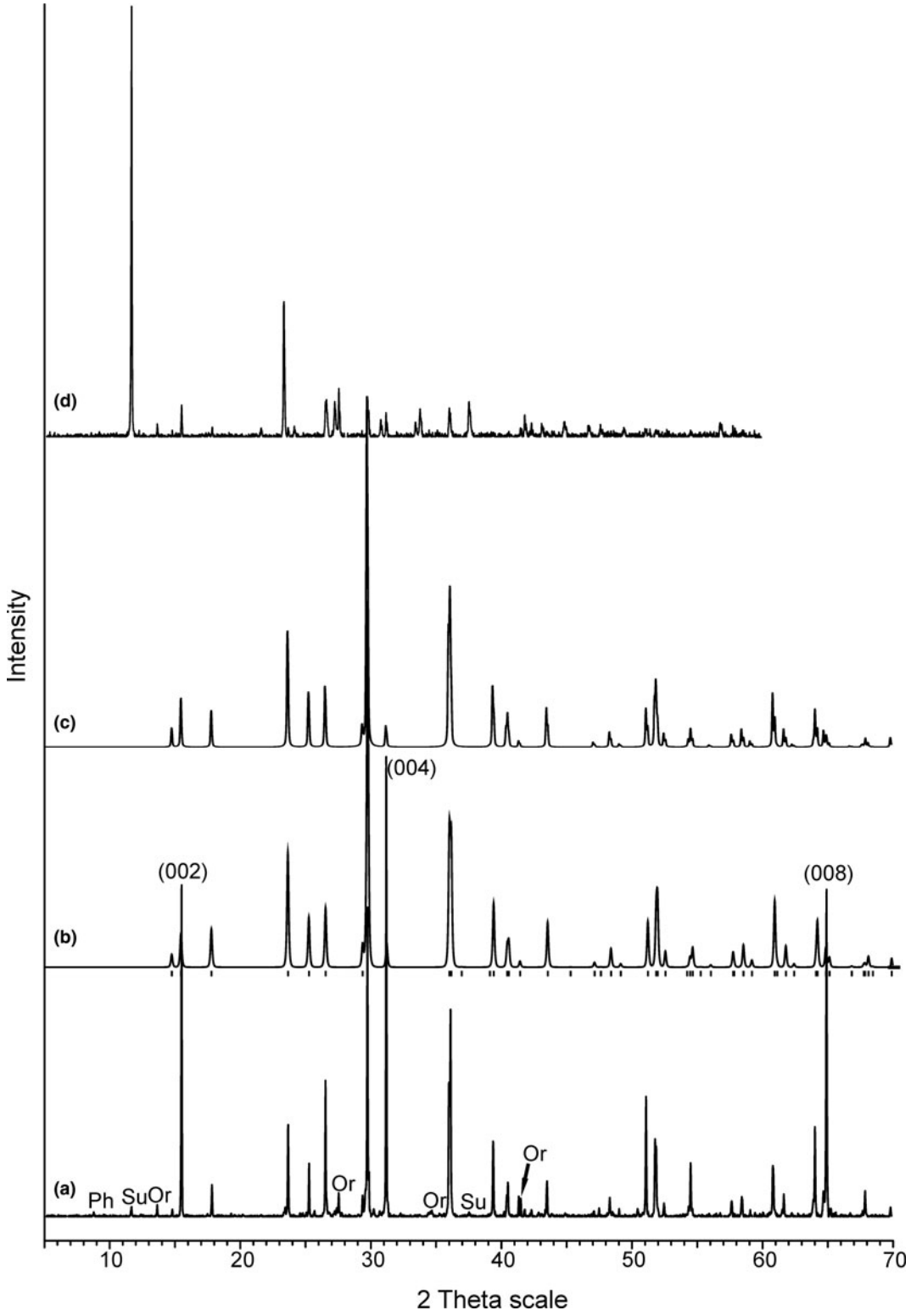


Fig. 3. The powder X-ray patterns (Cu*K*α, 40 kV and 40 mA) of: (*a*) bavsiite, measured with impurities of feldspar (Or), suzukiite (Su) and mica (Ph) – note the preferred orientation effects on the (00*l*) reflections in the experimental pattern of bavsiite; (*b*) calculated powder pattern of bavsiite with data from structure refinement; (*c*) calculated powder pattern of β-$BaVSi_2O_7$ with parameters of the structure refinement from Liu and Greedan (1994); and (*d*) suzukiite, $BaVSi_2O_7$, experimental pattern with crystals from the type locality of bavsiite.

and corrected for absorption using the program *SADABS* (Bruker, 2008). The analyses of the intensity data indicate the two possible space groups *I*4/*m* and *I*4/*mmm*. The merged intensities for *I*4/*m* result in $R_{int} = 0.033$, $\sigma = 0.015$ and for *I*4/*mmm* in $R_{int} = 0.062$, $\sigma = 0.018$. For bavsiite we adopted as a starting point the space group *I*4/*m* and the atomic positions as reported for the structural

https://doi.org/10.1180/mgm.2019.59 Published online by Cambridge University Press

Table 4. Crystal parameters, data collection and structure refinement details for bavsiite.

Crystal data	
Ideal formula	$Ba_2V_2O_2[Si_4O_{12}]$
Crystal size (mm)	0.15 × 0.11 × 0.04
Crystal system, space group	Tetragonal, *I*4/*m*
Formula weight	712.92
Temperature (K)	100
Unit-cell dimensions (Å)	a = 7.043(1), c = 11.444(2)
V (Å^3)	567.6(2)
Z	2
Density (from above formula) (g/cm^3)	4.171
Absorption coefficient (mm^{-1})	8.95
Data collection	
Description	Medium blue, platy crystal
Instrument	Bruker AXS Smart Apex CCD
Radiation type, wavelength (Å)	Mo$K\alpha$, 0.71073 Å
F(000)	652
θ range	3.40 to 26.28°
Index ranges	$-8 \le h \le 8$, $-8 \le k \le 8$, $-14 \le l \le 14$
Reflections collected/unique	2287/312
R_{int}, R_σ	0.033, 0.015
Ratio of min. to max. transmission	0.636
Refinement	
Refinement method	Full-matrix least-squares on F^2
Data / restraints / parameters	312 / 0 / 32
Twinning by merohedry	010/100/00$\bar{1}$
BASF parameter	0.290(4)
Extinction	0.0027(4)
Final R indices [$I > 2\sigma(I)$] (all data)	R_1 = 0.0159, wR_2 = 0.0399 (312 data)
GoF on F^2	1.175
Largest diff. peak and hole (e^-Å^{-3})	0.37 and −0.47

$R_1 = \Sigma||F_o|-|F_c||/\Sigma|F_o|$, $wR_2 = [\Sigma(w(F_o^2-F_c^2)^2)/\Sigma(w(F_o^2)^2)]^{½}$
$w = 1/[\sigma^2(F_o^2)+(0.0179P)^2+2.33P]$, $P=(Max(F_o^2,0) + 2F_c^2)/3$

Table 6. Selected bond distances (Å) and angles (°) in bavsiite.

Ba–O(1) ×4	3.295(2)	O(2)–V–O(3) ×4	103.29(8)
Ba–O(2) ×4	2.812(4)	O(2)–V–O(2)′ ×2	153.4(2)
Ba–O(2)′ ×4	3.149(4)	O(2)–V–O(2)″ ×4	86.97(4)
Ba–O(3) ×4	3.562(5)		
		O(1)–Si–O(1)′	112.1(3)
V–O(2) ×4	1.951(3)	O(1)–Si–O(2)′ ×2	106.6(2)
V–O(3)	1.608(5)	O(1)′–Si–O(2)′ ×2	108.5(2)
		O(2)–Si–O(2)′	114.6(2)
		<O–Si–O>	109.5
Si–O(1)	1.609(5)		
Si–O(1)′	1.616(5)	Si–O(1)–Si′ ×4	157.9(5)
Si–O(2) ×2	1.594(3)		
<Si–O>	1.603	Shortest O⋯⋯O	2.569

identic synthetic phase β-$BaVSi_2O_7$ by Liu and Greedan (1994). The small amounts of titanium and iron in the empirical formula of bavsiite (Table 2) were summarised with full occupancy of vanadium at the V site and all other sites were expected to be fully occupied by silicon, barium and oxygen, respectively. Least-squares structure refinement using anisotropic displacement parameters for all atoms was carried out with the program *SHELXL-2013* (Sheldrick, 2015). It converged at satisfactory R values (R_1 = 0.0279) but the second parameter in the weighting scheme was unusually large (17.98). Refinement with space group *I*4/*mmm* gave nearly the same values for atomic positions and anisotropic displacement parameters but with slightly higher R values (R_1 = 0.0323) and also an unusually large second weighting parameter (24.32). These results are an indication of a twinning effect in the crystal structure of bavsiite. No splitting of reflections in the data collection was observed, thus a twinning by merohedry is predicted. In Laue group 4/*m* a mirror *m* parallel to the fourfold axis acts as a twin element and the apparent Laue group 4/*mmm* results. The refinement with space group *I*4/*m* using the twinning law 010/100/00$\bar{1}$ confirmed the merohedral twinning effect by lowering R_1 to 0.0159 and the presence of twin domains with proportions 0.29 to 0.71. In addition, the weighting scheme shows acceptable values (WGHT 0.0179, 2.33) and a smooth difference-Fourier map shows that absorption effects are well corrected.

Details on data collection, crystallographic data and refinement are given in Table 4. Refined atomic coordinates and displacement parameters are given in Table 5, and selected interatomic distances and angles are listed in Table 6. Bond valences (Table 7) were calculated using the equation of Brown and Altermatt (1985) with the parameters of Gagné and Hawthorne (2015). The crystallographic information files have been deposited with the Principal Editor of *Mineralogical Magazine* and are available as Supplementary material (see below).

Description of the crystal structure

Bavsiite, $Ba_2V_2O_2[Si_4O_{12}]$, crystallises in a tetragonal unit cell of space group *I*4/m with one of the oxygen atoms in a general position whereas all other sites are located at special positions (Table 5). The structure can be considered as consisting of unbranched single $[Si_4O_{12}]^{8-}$ rings connected by $[VO_5]^{6-}$ square pyramids (Fig. 4), or of cage–like $[Si_4V_2O_{18}]^{12-}$ clusters built by four $[SiO_4]^{4-}$ tetrahedra and two $[VO_5]^{6-}$ square pyramids (Fig. 5). These clusters are cross-linked to form a pseudo-two-dimensional network (2D) parallel to (001) containing empty channels along the *a* axis as shown in Fig. 6. There is no connection between the $[VO_5]^{6-}$ square pyramids by themselves and the V–V distance of 3.580 Å sets an upper limit for the channel height (Fig. 6). The 2D networks are held together by Ba^{2+} ions located in channels parallel to the *c* axis (Fig. 7).

The Si–O bond length ranges from 1.594(3) to 1.616(5) Å, average 1.603 Å, and the O–Si–O angles from 106.6(2)° to 114.6(2)°,

Table 5. Atomic coordinates, equivalent isotropic and anisotropic displacement parameters (Å^2) for bavsiite.

Atom	x	y	z	U_{eq}	U^{11}	U^{22}	U^{33}	U^{23}	U^{13}	U^{12}
Ba	½	0	¼	0.0117(2)	0.0130(2)	0.0130(2)	0.0093(2)	0	0	0
V	0	0	0.3436(1)	0.0078(3)	0.0081(3)	0.0081(3)	0.0072(5)	0	0	0
Si	0.2119(2)	0.2369(2)	0	0.0066(3)	0.0052(7)	0.0055(7)	0.0091(6)	0	0	0.0014(5)
O(1)	0.2682(5)	0.0144(7)	0	0.0283(10)	0.011(2)	0.008(2)	0.065(3)	0	0	0.003(2)
O(2)	0.2098(5)	0.1693(5)	0.3828(2)	0.0280(9)	0.028(2)	0.040(2)	0.016(1)	−0.013(1)	0.007(1)	−0.023(2)
O(3)	0	0	0.2031(4)	0.0165(10)	0.018(2)	0.018(2)	0.014(2)	0	0	0

U_{eq} is defined as one third of the trace of the orthogonalised U_{ij} tensor.
The anisotropic displacement factor exponent takes the form: $-2\pi^2$ [$h^2a^{*2}U^{11}+\ldots+2hka^*b^*U^{12}$]

https://doi.org/10.1180/mgm.2019.59 Published online by Cambridge University Press

Table 7. Bond-valence sums in valence units (vu) for bavsiite.

	Ba	V	Si	Σ
O(1)	0.07 ×4		1.04 1.02	2.20
O(2)	0.23 ×4 0.10 ×4	0.62×4	1.08 ×2	2.03
O(3)	(0.04 ×4)	1.59		1.59 (1.75)
Σ	1.60 (1.76)	4.07	4.22	

Bonds for O(1): 2 × Si + 2 × Ba; O(2): 1× Si + 1 × V + 2 × Ba; O(3): 1 × V + (4 × Ba)

average 109.5°, indicating a nearly regular tetrahedron. The bond angles of the unbranched $[Si_4O_{12}]^{8-}$ ring are 112.1(3)° for O(1)–Si–O(1)' and 157.9(5)° (= 270° – 112.1°) for Si–O(1)–Si'.

Vanadium occurs in a distorted square pyramidal oxygen environment with equatorial bond length of 1.951(3) Å and a very short axial one of 1.608(5) Å. The displacement of the central V atom off the basal square plane towards the axial oxygen O(3) is indicated by the O(2)–V–O(3) basal to axial oxygen angle of 103.29(8)° and is also visible in Fig. 4.

Ions of Ba^{2+} occupy channels along c and can be considered as 12-coordinated with Ba–O bond lengths ranging from 2.812(4) to 3.295(2) Å and an average of 3.085 Å. A further but very long Ba–O distance of 3.562(5) Å would sum to a 16-coordination with an even longer average length of 3.205 Å.

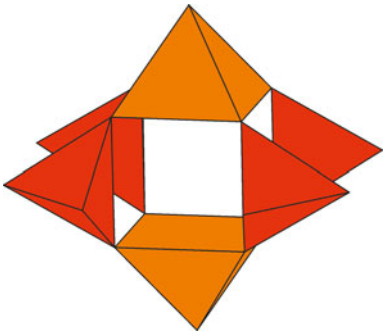


Fig. 5. The cage-like $[Si_4V_2O_{18}]^{12-}$ cluster is a basic structural unit of bavsiite. The $[SiO_4]$ tetrahedra are coloured red and $[VO_5]$ square pyramids brown.

Discussion

In the unbranched single $[Si_4O_{12}]^{8-}$ ring the anisotropic parameter U^{33} of the bridging oxygen O(1) is significantly higher than U^{11} and U^{22} generated by the strong bonding to two Si (Si–O(1) = 1.609(5) Å and Si–O(1)' = 1.616(5) Å) in the plane Si–O(1)–Si' parallel to (001) and loosely bonding to two Ba ions (Ba–O(1) = 3.295(2) Å) with c-axis–Ba–O(1) = 29.75° with respect to U^{33}. The silicon tetrahedron in bavsiite is more regular than in β-$BaVSi_2O_7$ [Si–O(1) = 1.622(5) Å, Si–O(1)' = 1.597(5) Å and 2× Si–O(2) = 1.603 Å] with Si–O averages of 1.603 Å (bavsiite) and 1.606 Å, respectively. The bond-valence sum in bavsiite for the tetrahedrally coordinated O(1) is high (V = 2.20) whereas the value for O(2) is nearly ideal (V = 2.03). O(2) connects the silicon tetrahedron with the $[VO_5]^{6-}$ square pyramid and has an additional two bonds with Ba. Such square pyramids are important structure elements in similar silicates such as β-$BaVSi_2O_7$, (Liu and Greedan, 1994), suzukiite, $BaVSi_2O_7$ (Ito *et al.*, 2014), haradaite, $SrVSi_2O_7$ (Basso *et al.*, 1995) and synthetic

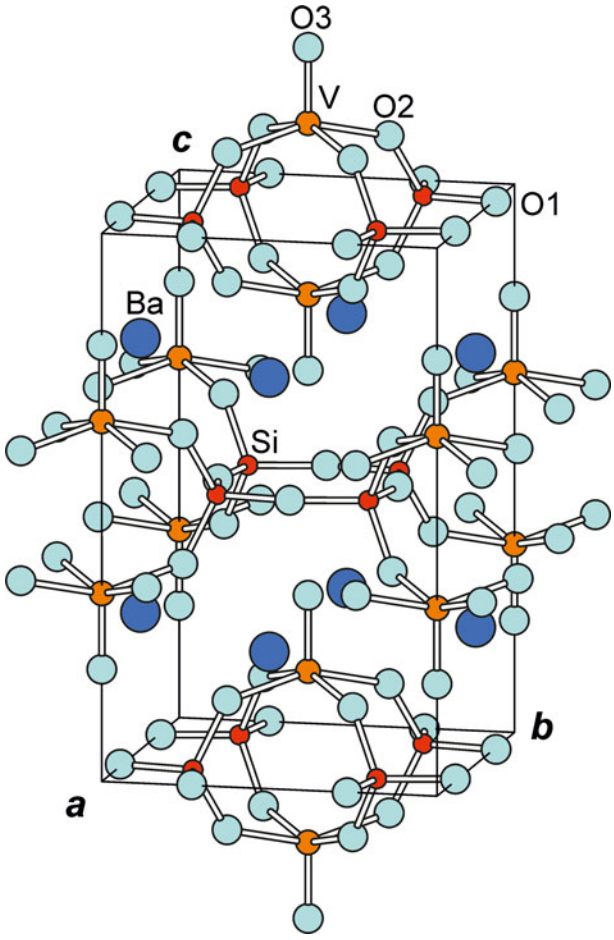


Fig. 4. Inclined projection of the crystal structure of bavsiite. Ba–O bonds are omitted for clarity.

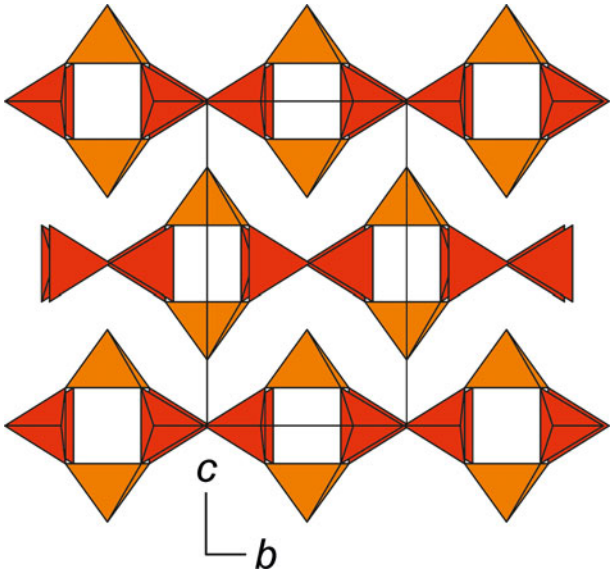


Fig. 6. The cross-linked clusters form a pseudo-two-dimensional network parallel to (001) containing empty channels along the *a* axis. Ba atoms are omitted for clarity.

https://doi.org/10.1180/mgm.2019.59 Published online by Cambridge University Press

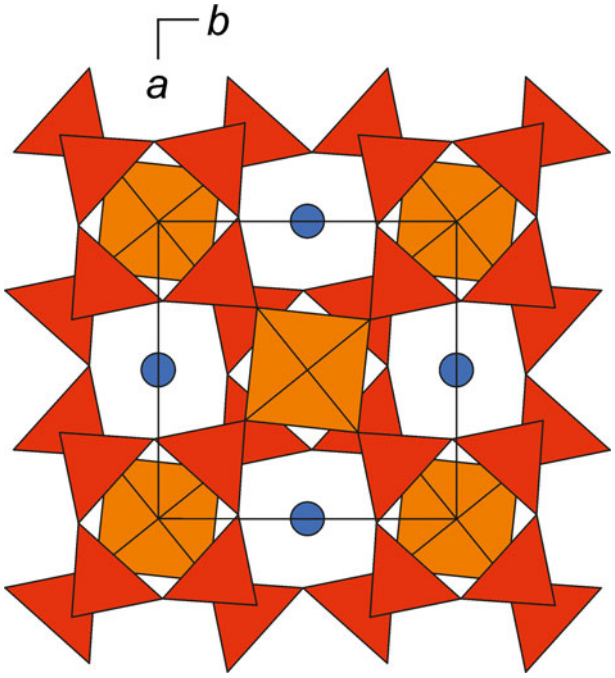


Fig. 7. The crystal structure of bavsiite projected along [001] with Ba atoms (blue circles) in the channels along *c*.

$SrVSi_2O_7$ (Berger and Range, 1996). In the $[VO_5]^{6-}$ square pyramid two types of bonds are visible by their V–O distances: (1) a very short vanadyl bond (shorter than 1.74 Å) and (2) longer equatorial bonds in ($V^{4+}O_n$) polyhedra in the range 1.90 to 2.12 Å (Schindler *et al.*, 2000). In bavsiite the vanadyl bond V–(O3) = 1.608(5) Å is longer than in β–$BaVSi_2O_7$, suzukiite and haradaite but nearly equal as in synthetic $SrVSi_2O_7$: 1.592 (8) Å, 1.593(5) Å, 1.593(9) Å and 1.61(1) Å, respectively. The equatorial bonds in bavsiite and β–$BaVSi_2O_7$, (1.951(3) Å and 1.936(5) Å, respectively) are shorter than in suzukiite, haradaite and synthetic $SrVSi_2O_7$ (1.9986(19) Å, 1.990(4) Å and 1.980(5) Å, respectively). In bavsiite the bond-valence sum 1.59 valence units (vu) for O(3) reflects the double bond nature of the vanadyl bond. The nearest further cation bond is to Ba with 3.562(5) Å and would increase the valence value to 1.75 vu for O(3).

The tight bonds in the $[Si_4V_2O_{18}]^{12-}$ cluster result in high valence values for Si and V (4.22 and 4.07 vu, respectively) whereas the Ba atoms in the channels along the c axis are only loosely bonded with valence sums of 1.60 vu (12-coordinated) or 1.76 vu (16-coordinated). The good cleavage in bavsiite parallel to (001), also visible by preferred orientation reflexes (00*l*) in the powder X-ray pattern (Fig. 3), is mainly due to the lengthened Ba–O bonds, which hold together the 2D-network.

According to Strunz and Nickel (2001) bavsiite is a cyclosilicate with 4-membered single rings (9.CF.). Bavsiite is isotypic to synthetic β-$BaVSi_2O_7$ (Liu and Greedan, 1994) and polymorphic to suzukiite, $BaVSi_2O_7$. In the crystal structure of suzukiite (Ito *et al.*, 2014) SiO_4 tetrahedra are connected to corrugated Si_4O_{12} chains along the *c* axis and VO_5 square pyramids link the chains to form layers parallel to the *ac* plane, which are connected by barium atoms.

Supplementary material. To view supplementary material for this article, please visit https://doi.org/10.1180/mgm.2019.59

Acknowledgements. We are grateful to Stuart Mills for editorial handling and helpful comments and Gunnar Färber, Germany, who provided the bavsiite-bearing samples. The comments of Peter Leverett and two anonymous reviewers improved the manuscript substantially.

References

Alfors J.T. and Pabst A. (1984) Titanian taramellites in western North America. *American Mineralogist*, **69**, 358–373.

Basso R., Lucchetti G., Palenzona A. and Zefiro L. (1995) Haradaite from the Gambatesa mine, eastern Liguria, Italy. *Neues Jahrbuch für Mineralogie – Monatshefte*, **6**, 281–288.

Berger T. and Range K.–J. (1996) Zwei Metasilicate mit Vierer-einfach-Ketten: Hochdrucksynthese und Strukturverfeinerung von $Sr_2(VO)_2Si_4O_{12}$ (Haradait) und $Sr_2(TiO)_2Si_4O_{12}$. *Zeitschrift für Naturforschung, Teil B. Anorganische Chemie, Organische Chemie*, **51**, 1099–1103.

Bojar H.-P. and Walter F. (2014) Bavsiite, IMA 2014-019. CNMNC Newsletter No. 21, August 2014, page 800; *Mineralogical Magazine*, **78**, 797–804.

Brown I.D. and Altermatt D. (1985) Bond-valence parameters obtained from a systematic analysis of the Inorganic Crystal Structure Database. *Acta Crystallographica*, **B41**, 244–247.

Bruker (2008) *Programs SMART, SAINT, SADABS, XPREP,* and *SHELXTL*. Bruker AXS Inc., Madison, Wisconsin, USA.

Bruker-AXS (2009) *TOPAS Software User Manual Version 4.2*. Karlsruhe, Germany.

Gagné O.C. and Hawthorne F.C. (2015) Comprehensive derivation of bond–valence parameters for ion pairs involving oxygen. *Acta Crystallographica*, **B71**, 562–578.

Ito M., Matsubara S., Yokoyama K., Momma K., Miyawaki R., Nakai I. and Kato A. (2014) Crystal structure of suzukiite from the Mogurazawa mine, Gunma Prefecture, Japan. *Journal of Mineralogical and Petrological Sciences*, **109**, 222–227.

Kampf A.R., Peterson R.C. and Joy B.R. (2014) Itsiite, $Ba_2Ca(BSi_2O_7)_2$, a new mineral species from Yukon, Canada: description and crystal structure. *The Canadian Mineralogist*, **52**, 401–407.

Liu G. and Greedan J.E. (1994) Crystal structure and magnetic properties of $BaVSi_2O_7$. *Journal of Solid State Chemistry*, **108**, 267–274.

MacNeil L.A., Peterson R.C., Färber G, Groat L. and Witzke T. (2013) Mineralogical studies of a low-temperature hydrothermal barium-rich skarn deposit, Gunn Claim, Yukon Territory. *Winnipeg 2013: GAC–MAC Joint Annual Meeting*. Abstract volume, **135**, p. 135.

Montgomery J.H., Thompson R.M. and Meagher E.P. (1972) Pellyite, a new barium silicate mineral from the Yukon Territory. *The Canadian Mineralogist*, **11**, 444–447.

Peterson R.C., Färber G., Evans R.J., Groat L., MacNeil L., Joy B., Lafuente B. and Witzke T. (2016) Meierite, a new barium mineral with a KFI-type zeolite framework from the Gun Claim, Yukon Canada. *The Canadian Mineralogist*, **54**, 1249–1259.

Pouchou J.L. and Pichoir F. (1991) Quantitative analysis of homogeneous or stratified microvolumes applying the model 'PAP'. Pp. 31–75 in: *Electron Probe Quantitation* (K.F.J. Heinrich and D.E. Newbury, editors). Plenum Press, New York.

Schindler M., Hawthorne F.C. and Baur W.H. (2000) Crystal chemical aspects of vanadium: polyhedral geometries, characteristic bond valences, and polymerization of (VO_n) Polyhedra. *Chemistry of Materials*, **12**, 1248–1259.

Sheldrick G.M. (2015) Crystal structure refinement with SHELXL. *Acta Crystallographica*, **C71**, 3–8.

Strunz H. and Nickel E.H. (2001) *Strunz Mineralogical Tables*. Schweizerbart´sche Verlagsbuchhandlung, Stuttgart, Germany, 870 pp.